

## Analysis of $p$ - $p$ Data Near the Interference Minimum\*†

MARTIN L. GURSKY AND LEON HELLER

*University of California, Los Alamos Scientific Laboratory, Los Alamos, New Mexico*

(Received 3 August 1964)

In the first part of this paper  $p$ - $p$  elastic scattering data at 90°c.m. near the Coulomb-nuclear interference minimum are analyzed. The energy of the minimum of the 90° cross section is found to be at 0.38243 ± 0.00020 MeV. The nuclear  $s$ -wave phase shift, defined with respect to wave functions which solve the Coulomb plus vacuum polarization potential problem, is found to be  $\delta_0^p = 0.25501 \pm 0.00020$ , at the precise energy 0.38243 MeV. In the second part of the paper the phase shift just obtained is used, in conjunction with four very accurate phase shifts from 1.4 to 3.0 MeV, to determine the parameters of the  $s$ -wave effective-range expansion. If this expansion is cut off after three terms (quadratic fit) then the scattering length is found to be  $a = -7.815 \pm 0.008$  F; the effective range  $r_0 = 2.795 \pm 0.025$  F; and the shape-dependent parameter  $P = 0.028 \pm 0.014$ . However, it is argued that the first three coefficients in the actual power-series expansion of the effective-range function are not known this well, and in particular,  $P$  may be very different from the actual coefficient occurring in the  $k^4$  term.

### I. INTRODUCTION

THE recent availability of very accurate low-energy proton-proton cross-section data makes it possible to determine the energy dependence of the  $s$ -wave phase shift to a considerably greater accuracy than before, and in particular to determine the curvature of the effective range function plotted versus energy.

In the first part of this paper (II)  $p$ - $p$  cross section data<sup>1,2</sup> at 90°c.m. near the Coulomb nuclear interference minimum are analyzed. The data are summarized in Sec. II A and a brief account of the theory presented in Sec. II B. The method used to take into account the geometry of the experiment and multiple scattering in the gas is discussed in Sec. II C. Section II D merely states that molecular effects are completely negligible even though they do smear out the center-of-mass energy. In Sec. II E, the results of the analysis of the experiment<sup>1</sup> are presented.

In part III, the phase shift obtained in part II is used in conjunction with accurate low-energy  $s$ -wave phase shifts obtained from Wisconsin data<sup>3,4</sup> to examine the energy dependence of the  $s$ -wave phase shift. The scattering length, effective range, and shape-dependent parameter are evaluated using a quadratic fit to the effective range function, and a discussion is presented of the relation between these parameters and the actual coefficients of the power series expansion of that function.

Appendix A presents some empirical formulas for the vacuum polarization quantities which are used in the

analysis, and Appendix B contains a simple discussion of the Coulomb plus  $s$ -wave nuclear amplitude at 90°c.m.

### II. ANALYSIS OF LOS ALAMOS EXPERIMENT

#### A. Summary of Experimental Results to be Analyzed

The experiment which provided the data for the low-energy analysis of this paper has been described in detail elsewhere.<sup>1</sup> Basically, it consisted of a coincidence measurement of the elastic cross section at 90°c.m. at several energies near the interference minimum (see Fig. 1).

The resulting data are presented, along with the errors associated therewith, in Table I. These numbers were obtained from Table I of Ref. 1.  $N(E)$  represents the number of coincidences per unit incident charge, and hence has the significance of a relative cross section. Since no attempt was made to measure the temperature of the target hydrogen,<sup>1</sup> its density is not well known, and therefore comparisons with the absolute value of the cross section cannot be made accurately. In Sec. E such a comparison is discussed nevertheless, and it is shown that there is no contradiction.

As discussed in Ref. 1, there is reason to believe that the data at 0.37283 MeV are not as reliable as the error quoted for it (due mainly to statistics) might indicate. With this in mind we have performed the analysis both with and without this point included. The difference between these two sets of results will be displayed later on.

#### B. Theory

Proton-proton effective range theory with explicit inclusion of vacuum polarization effects has been treated earlier by Heller.<sup>5</sup> We shall here summarize the principal results of that work using similar notation.

The unsymmetrized scattering amplitude (in the

\* Work done under the auspices of the U. S. Atomic Energy Commission.

† Preliminary accounts of this work were reported at the Pasadena and Tucson meetings of the American Physical Society [Bull. Am. Phys. Soc. 8, 605 (1963), and 9, 154 (1964)].

<sup>1</sup> J. E. Brolley, Jr., J. D. Seagrave, and J. G. Beery, Phys. Rev. 135, B1119 (1964).

<sup>2</sup> A similar experiment with less precision was performed by D. L. Cooper, D. H. Frisch and R. L. Zimmerman, Phys. Rev. 94, 1209 (1954).

<sup>3</sup> D. J. Knecht, S. Messelt, E. D. Berners, and L. C. Northcliffe, Phys. Rev. 114, 550 (1959) and more recent data to be published (private communication from P. F. Dahl and D. J. Knecht).

<sup>4</sup> H. P. Noyes, Phys. Rev. Letters 12, 171 (1964).

<sup>5</sup> L. Heller, Phys. Rev. 120, 627 (1960).

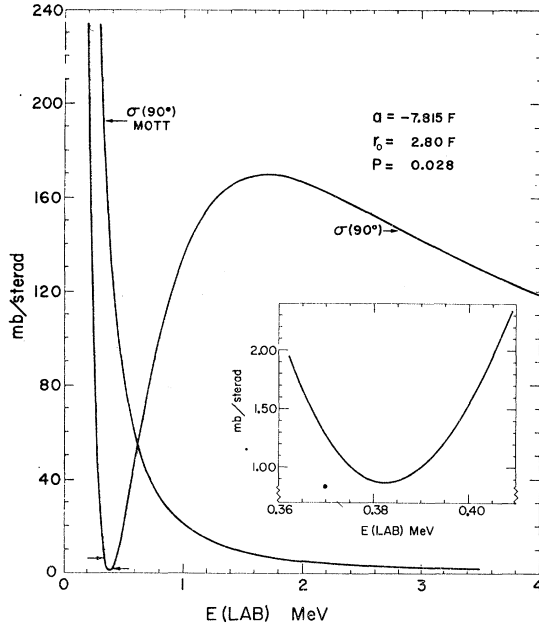


FIG. 1. Center-of-mass differential cross section at  $90^\circ$  versus the laboratory energy of the incident proton. The Mott cross section is shown and the actual cross section computed from the parameters which are found in Part II to give the best quadratic fit to the effective range function. The region between the two arrows is the energy range of the experiment (Ref. 1) being analyzed in Part I. The insert shows the region near the minimum in greater detail.

c.m. system) is given as the sum of three terms

$$f(\theta) = f_c(\theta) + f_{v.p.}(\theta) + f_N(\theta). \quad (1)$$

The cross section is obtained by symmetrizing (anti-symmetrizing) this amplitude in the singlet (triplet) state, and adding  $\frac{1}{4}$  of the singlet cross section to  $\frac{3}{4}$  of the triplet cross section.<sup>6</sup>

The ordinary Coulomb amplitude is given by

$$f_c(\theta) = \frac{-\eta}{2k \sin^2(\theta/2)} e^{-2i\eta \ln \sin(\theta/2)}, \quad (2)$$

with

$$\eta = e^2/\hbar v,$$

where  $v$  is the laboratory velocity of the incident proton,<sup>7</sup> and

$$k = (ME_{\text{lab}}/2\hbar^2)^{1/2}$$

with  $M$  the proton mass.

<sup>6</sup> In Ref. 5, for illustrative purposes, the symmetrized singlet cross section was written out explicitly with the approximation that the term  $|f_{v.p.}|^2$  is negligible. Since in this experiment  $f_c$  and  $f_N$  cancel each other to a very great extent, one should not make that approximation.

<sup>7</sup> We have adopted a suggestion of G. Breit, Rev. Mod. Phys. 34, 766 (1962), and computed  $\eta$  in this manner, using the correct relativistic velocity of the incident proton. As expected, and demonstrated later on, this relativistic effect is almost completely negligible at this energy.

TABLE I. Relative cross sections measured at six energies.<sup>a</sup>

$E$ (MeV)	$N(E)$ (arbitrary units)
0.33766	$52.420 \pm 0.847$
0.36248	$16.285 \pm 0.155$
0.37283	$10.614 \pm 0.159$
0.38348	$8.280 \pm 0.093$
0.39425	$10.307 \pm 0.088$
0.40517	$16.363 \pm 0.139$

<sup>a</sup> Reference 1.

The amplitude which describes the effect of vacuum polarization is used in the form

$$f_{v.p.} = (1/k) \sum_L (2L+1) \tau_L e^{2i(\sigma_L - \sigma_0)} P_L(\cos\theta), \quad (3)$$

where  $\tau_L$ , the vacuum polarization phase shift, is much less than unity and  $\sigma_L$  is the Coulomb phase shift. We designate the Coulomb plus vacuum polarization potentials as the 'electric' potential, and the wave functions which solve that problem as the electric functions.

The nuclear amplitude in general is given by

$$f_N = (1/2ik) \sum_L (2L+1) e^{2i(\sigma_L - \sigma_0)} \times e^{2i\tau_L} (e^{2i\delta_L^E} - 1) P_L(\cos\theta), \quad (4)$$

where  $\delta_L^E$  is the nuclear phase shift defined with respect to the electric functions. The superscript  $E$  is used on the phase shift defined in this way throughout the paper.

We assume that the only nuclear contribution to the singlet amplitude comes from  $L=0$ , and thus we take

$$f_N(\theta) = e^{i\delta_0^E} \sin\delta_0^E e^{2i\tau_0}/k. \quad (5)$$

We have computed the  $d$ -wave amplitude predicted by one pion exchange and find that it is completely negligible (even though the nuclear and Coulomb singlet amplitudes cancel each other to a considerable extent). The three  $p$ -wave phase shifts were computed as in Ref. 4 with the additional simplification that the linear combination which is proportional to the strength of the central force plays no role at  $90^\circ$ , i.e., we include only the one-pion-exchange tensor force. We find it is completely negligible, and would still be if the tensor force were four times as strong.

The dependence of  $\delta_0^E$  on energy is represented by an expansion of the effective range function. This function (treating vacuum polarization to first order) and its expansion are given by

$$X(k) \equiv C^2 k [(1+2X_0) \cot\delta_0^E - \tau_0] + 2\eta k [h(\eta) + l_0(\eta)] \\ = -\frac{1}{a} + \frac{1}{2} r_0 k^2 - P r_0^3 k^4 + Q r_0^5 k^6 - \dots \quad (6)$$

The quantities  $\tau_0$ ,  $X_0$ , and  $l_0$  are defined in terms of the

electric functions in Ref. 5, and were computed as a first-order perturbation and plotted versus energy in that reference. In Appendix A empirical formulas are presented for these quantities and for the vacuum polarization scattering amplitude as well.  $h(\eta)$  is the same function which appears in the more common effective range expansion<sup>8</sup> for nuclear phase shifts defined with respect to Coulomb functions:

$$h(\eta) = \frac{1}{2} \left[ \frac{\Gamma'(-i\eta)}{\Gamma(-i\eta)} + \frac{\Gamma'(i\eta)}{\Gamma(i\eta)} \right] - \ln \eta.$$

The parameters  $a$ ,  $r_0$ , and  $P$  are commonly referred to as the effective range, scattering length, and shape-dependent parameter. Also

$$C^2 = 2\pi\eta / (e^{2\pi\eta} - 1).$$

The reason for choosing the interference minimum as the energy region for doing an experiment is that the great cancellation which occurs between Coulomb and nuclear amplitudes (see Fig. 1 and Appendix B) makes it possible with just a modest accuracy in the cross section, like 1%, to determine the  $s$ -wave phase shift to  $\sim 0.1\%$ . See Ref. 8, pp. 100-102 and references cited therein for more discussion of this question.

As we now show, in this energy region the cross section is determined almost completely by a single quantity,  $E_{\min}$ , the energy at the minimum of the 90° cross section. At these energies the differential cross section at 90° c.m. is a function of the energy, and of the  $s$ -wave phase shift  $\delta$ , which is itself a function of the energy and the effective range parameters which we designate collectively by  $\alpha$ .

$$\sigma = \sigma(E, \delta). \quad (7)$$

This implies for the first derivative with respect to energy

$$\frac{d\sigma}{dE} = \frac{\partial\sigma}{\partial E}(E, \delta) + \frac{\partial\sigma}{\partial\delta}(E, \delta) \frac{\partial\delta}{\partial E}(E, \alpha),$$

where the variables in parentheses are the ones upon which the corresponding functions depend.

Writing Eq. (6) as

$$X(\delta, E) = \beta + \gamma E + \mu E^2 + \dots,$$

where  $\beta$ ,  $\gamma$ , and  $\mu$  are simply related to the parameters  $\alpha$ , and differentiating with respect to  $E$  gives

$$\frac{\partial X}{\partial E}(E, \delta) + \frac{\partial X}{\partial\delta}(E, \delta) \frac{\partial\delta}{\partial E} = \gamma + 2\mu E + \dots$$

Using approximate values for the effective range parameters, some of which are already known well from previous experiments and others bracketed by theory,

<sup>8</sup> J. D. Jackson and J. M. Blatt, Rev. Mod. Phys. 22, 96 (1950).

it turns out that at the energies of this experiment

$$|\gamma + 2\mu E + \dots| \ll \left| \frac{\partial X}{\partial E} \right|$$

giving the result that

$$\frac{\partial\delta}{\partial E} \approx - \frac{\partial X}{\partial E}(E, \delta) / \frac{\partial X}{\partial\delta}(E, \delta) = f(E, \delta).$$

Thus, it follows that

$$\frac{d\sigma}{dE} \approx g(E, \delta), \quad (8)$$

and the use of identical arguments shows that all derivatives of  $\sigma$  with respect to energy are functions only of  $E$  and  $\delta$ , with no other dependence upon the parameters. Expanding  $\sigma$  about  $E_{\min}$ , all derivatives evaluated at  $E_{\min}$  become functions of  $E_{\min}$  and  $\delta(E_{\min}) \equiv \delta_{\min}$ . In addition the total derivative in (8) must vanish at  $E_{\min}$ , by definition of  $E_{\min}$ . This condition imposes a functional dependence of  $\delta_{\min}$  upon  $E_{\min}$ . Hence the principal parameter defining the cross section in this energy region is  $E_{\min}$ . If just the 90° Coulomb amplitude and the  $s$ -wave nuclear amplitude are included in the analysis, the relation between  $\delta_{\min}$  and  $E_{\min}$  can be pursued somewhat further. In Appendix B this is discussed briefly.

However, with vacuum polarization included, the explicit dependence of  $\sigma$  upon  $E_{\min}$  (and such other parameters as may enter in a minor way) is not easily obtained. On the basis of numerical calculations it can be determined that to a high degree of accuracy

$$E_{\min}(\text{MeV}) = 0.66463 + 0.03800a + 0.00530r_0.$$

This is valid for  $P=0$ , but the spread in  $E_{\min}$  obtained by letting  $P$  vary over a wide range of reasonable values is less than 0.2 keV. This is a reflection of the fact that the term in the effective range expansion involving  $P$  is almost completely negligible at the energies of this experiment. The term involving  $Q$  is negligible. Since this is an approximation we prefer to define a new parameter exactly by

$$\mathcal{E} \equiv 0.66463 + 0.03800a + 0.00530r_0 \quad (9)$$

as well as an "orthogonal" parameter

$$\mathfrak{D} \equiv 0.03800r_0 - 0.00530a, \quad (10)$$

and carry out the analysis in terms of these two parameters and  $P$  instead of  $a$ ,  $r_0$ , and  $P$ . We expect that  $\mathcal{E}$  will be determined very well by the experiment,  $\mathfrak{D}$  rather poorly, and  $P$  not at all. We do not search on  $P$ . Instead,  $P$  is set equal to zero [as are all higher order terms in Eq. (6)], and later the effect of varying  $P$  over a wide range of values, from  $-0.05$  to  $+0.10$ , is considered. This range includes all values of  $P$  which are known to the authors to have ever been considered for

the proton-proton problem. In practice, after choosing a pair  $(\mathcal{E}, \mathfrak{D})$ , Eqs. (9) and (10) must be inverted to find  $(a, r_0)$  which are then put into Eq. (6) to determine  $\delta$ .

### C. Geometry and Multiple Scattering

Due to the finite size of the volume in which the scatterings occur and to the finite size of the detectors (see Fig. 3 in Ref. 1), the quantities measured (tabulated in Table I) include contributions from a small range of scattering angles around  $90^\circ$  c.m. Ignoring for the moment the role of multiple scattering (in causing somewhat the same effect), we take geometrical effects into account in the following manner.

The theoretical prediction for  $N(E, \alpha)$ , the number of counts recorded per incident proton is proportional to an integral over the scattering volume and detector solid angle of the theoretical differential cross section. The proportionality constant  $C$  converts cross section to number of counts and is independent of all relevant variables.

$$N(E, \alpha) = C \int S(E, \alpha, \theta_L) f(\mathbf{r}_p, \theta_L, \varphi_L) d^3 r_p d\varphi_L d\theta_L, \quad (11)$$

where  $S(E, \alpha, \theta_L) = (d\sigma/d\Omega)_{\text{lab}} \sin\theta_L$ . The variables  $\mathbf{r}_p$ ,  $\theta_L$ , and  $\varphi_L$  are, respectively, the location of the scattering event, and the polar and azimuthal angles in the lab system of one of the protons' resultant path. [The recoil proton angles are, of course,  $\frac{1}{2}\pi - \theta_L$ ,  $\varphi_L + \pi$ .] The energy dependence as well as dependence on other

parameters (symbolized by  $\alpha$ ) are contained in  $S(E, \alpha, \theta_L)$ .  $f(\mathbf{r}_p, \theta_L, \varphi_L)$  is a function of the geometry of the apparatus in that  $f=1$  if both scattered protons can traverse the slit system and result in a coincidence count;  $f=0$  if either proton cannot. The integral must be taken over ranges of values of  $\mathbf{r}_p$ ,  $\theta_L$ ,  $\varphi_L$  sufficiently broad to include all such values for which  $f=1$ .

The quantity

$$F(\theta_L) \equiv \int f(\mathbf{r}_p, \theta_L, \varphi_L) d^3 r_p d\varphi_L \quad (12)$$

which represents the angular weight function for the geometry of this experiment<sup>1</sup> is shown in Fig. 2.

Since  $S(E, \alpha, \theta_L)$  is symmetric about  $\theta_L = 45^\circ$ , and the range of scattering angles is small, we may write

$$S(E, \alpha, \theta_L) = S_0(E, \alpha) + S_2(E, \alpha) (\theta_L - 45^\circ)^2, \quad (13)$$

where  $S_0(E, \alpha) \equiv S(E, \alpha, 45^\circ)$ .

Hence

$$N(E, \alpha) = C [S_0(E, \alpha) I_0 + S_2(E, \alpha) I_2], \quad (14)$$

where

$$I_0 \equiv \int F(\theta_L) d\theta_L, \quad (15)$$

and

$$I_2 \equiv \int (\theta_L - 45^\circ)^2 F(\theta_L) d\theta_L. \quad (16)$$

Since  $I_0$  depends neither upon  $E$  nor  $\alpha$  we may write

$$N(E, \alpha) = C' S_0(E, \alpha) \left[ 1 + \frac{S_2(E, \alpha)}{S_0(E, \alpha)} \left( \frac{I_2}{I_0} \right) \right], \quad (17)$$

where  $I_2/I_0$  is simply the normalized second moment of  $F(\theta_L)$ . Also plotted in Fig. 2 is  $S(E, \alpha, \theta_L)$  at several energies for the values of the parameters which we will later find provide the best fit to the data.

We now ask if there exists an effective angle  $\theta_e$ , independent of  $E$  and  $\alpha$ , such that the value of  $S(E, \alpha, \theta_e)$  is proportional to  $N(E, \alpha)$  with the proportionality constant also independent of  $E$  and  $\alpha$ . Such an angle does exist, and can be found from its definition

$$C'' [S_0 + S_2(\theta_e - 45^\circ)^2] = [S_0 I_0 + S_2 I_2].$$

Choosing  $C'' = I_0$ ,

$$\theta_e = 45^\circ + (I_2/I_0)^{1/2}. \quad (18)$$

The use of the effective angle results in an accuracy for the integrated quantity  $N(E, \alpha)$  which is very much greater than the corresponding experimental accuracy. This result also justifies the use of the quadratic approximation of Eq. (13).

Before computing  $I_2/I_0$  from Eqs. (15) and (16), we first discuss the role played by multiple scattering, even though it is a very small effect for the physical conditions of the experiment.<sup>1</sup>

Since the multiple scattering in the apparatus smears

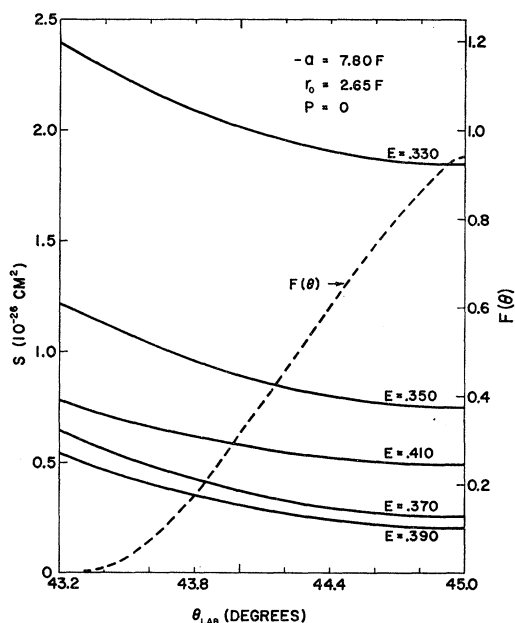


FIG. 2.  $F(\theta)$  is the angular weight function, in arbitrary units, for the geometry of the experiment (Ref. 1) being analyzed.  $S$  is the laboratory differential cross section multiplied by the sine function of the laboratory angle, computed at five equally spaced energies near the minimum, using the parameters  $(a, r_0)$  which are found in Part II to provide the best fit to the data.

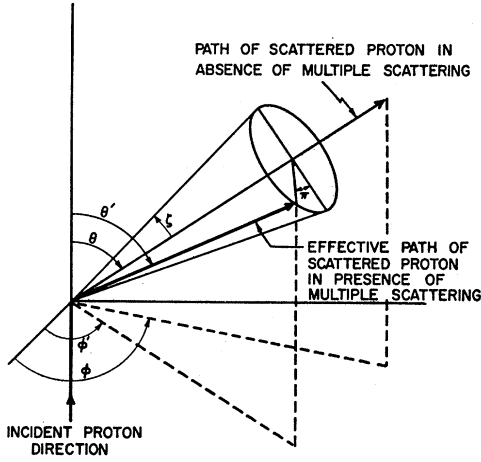


FIG. 3. The coordinates used to describe a scattering event and the effect of multiple scattering.

out the angular dependence of the observed results, it increases the quantity  $I_2/I_0$  in a way similar to that of finite geometry. Instead of arriving at the detector from the same direction ( $\theta_L, \varphi_L$ ) with which it left the point of scattering (see Fig. 3), the scattered proton now reaches the detector plane at a new point (and going in a new direction at that point, which however, is of no concern). Since the effect is small, we do not try to follow the actual path of the proton. Instead we employ the following model which provides an estimate of the effect of multiple scattering and which can be shown (for the slit system of this experiment) to result in an upper limit for  $I_2/I_0$ . We use a family of straight line "effective paths" which produces, at the detector, the same distribution of lateral displacements as that produced by the actual proton paths; i.e., we assume that the angular displacements ( $\zeta, \pi$ ) shown on Fig. 3 obey the probability distribution

$$P(\zeta, \pi) d\Omega = \exp[-(\zeta/\zeta_0)^2] \sin \zeta d\zeta d\pi,$$

where  $\zeta_0$  is the rms multiple scattering angle.

Now, instead of the function  $f(\mathbf{r}_p, \theta_L, \varphi_L)$  which described the geometry in the case of no multiple scattering, we have a function

$$f(\mathbf{r}_p, \theta_L, \varphi_L, \zeta_1, \pi_1, \zeta_2, \pi_2; \zeta_0)$$

occurring in the integrals (11) and (12). The integration is now taken over  $\mathbf{r}_p, \theta_L, \varphi_L, \zeta_1, \pi_1, \zeta_2, \pi_2$  with the subscripts on  $\zeta, \pi$  referring to the two scattered protons. The function  $f$  is evaluated analogously to the case of no multiple scattering: If the addition of  $\theta_L, \varphi_L$ , and  $\zeta_1, \pi_1$  results in angles  $\theta_{L1}', \varphi_{L1}'$ ; and the addition of  $(\pi/2) - \theta_L, \pi + \varphi_L$  and  $\zeta_2, \pi_2$  results in angles  $\theta_{L2}', \varphi_{L2}'$  such that the two protons both traverse the slit system, then the function  $f$  takes on the value of the probability of obtaining both  $\zeta_1$  and  $\zeta_2$ :

$$f = \sin \zeta_1 \sin \zeta_2 \exp[-(\zeta_1/\zeta_0)^2 - (\zeta_2/\zeta_0)^2].$$

If either of the protons cannot traverse the slit system,  $f=0$ .

From Eqs. (12), (15), and (16), the angular weight function  $F(\theta)$  and its normalized second moment  $I_2/I_0$ , are thus functions of  $\zeta_0$ . Shown in Fig. 4 is the sensitivity of  $I_2/I_0$  to variations in  $\zeta_0$  in the region of  $\zeta_0=0.05^\circ$ ; this is our best estimate<sup>9</sup> of  $\zeta_0$  for the geometry and state of the gas occupying the apparatus in the experiment,<sup>1</sup> but it is uncertain by a factor of 3. Although the integrals in Eqs. (12), (15), and (16) are in principle exactly determinable, the values in Fig. 4 reflect the fact that the multidimensional integrals were performed statistically using a Monte Carlo technique. It will be shown later that the complete spread of values of  $I_2/I_0$ , due both to the uncertainty in  $\zeta_0$  and to the limited accuracy of the integrations, is of almost negligible consequence.

Another related effect arises from the fact that the beam is not perfectly parallel but has a divergence<sup>1</sup> of  $0.055^\circ$ . The resultant smearing is comparable to that produced by multiple scattering and is satisfactorily included by taking the acceptable range of values for  $I_2/I_0$  to run from  $1.13 \times 10^{-4}$  to  $1.22 \times 10^{-4}$  (see Fig. 4).

Possible scattering by the slits<sup>10</sup> has a completely negligible effect upon  $I_2/I_0$ . Permitting a 200-keV proton to travel through a maximum of  $4 \times 10^{-5}$  cm of an iron slit—a larger distance produces so great an energy loss that it would not be counted even if it did reach the detector—broadens the angular weight function  $F(\theta)$  slightly, and also permits some new scattering angles (up to  $2.6^\circ$  different from  $45^\circ$ , see Fig. 3 in Ref. 1) to be detectable. We have determined that these two effects increase  $I_2/I_0$  by less than 1%.

The relativistic angle transformation (in place of the

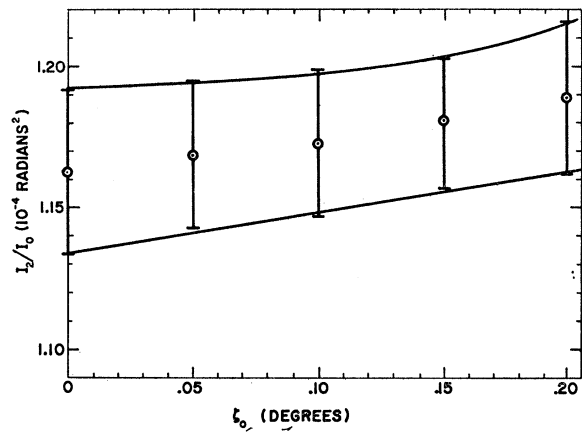


FIG. 4. The normalized second moment of the angular weight function versus the rms multiple scattering angle. The integrals defining  $I_0$  and  $I_2$  were performed by a Monte Carlo technique and the bars represent the uncertainties in the answers.

<sup>9</sup> See, for example, H. A. Bethe, Phys. Rev. 89, 1256 (1953).

<sup>10</sup> We thank Professor Breit for calling this question to our attention.

nonrelativistic one used above) can also be considered as an effect upon  $I_2/I_0$  which is completely negligible.

We adopt  $1.171 \times 10^{-4}$  as the best value of  $I_2/I_0$ , and this leads to an effective laboratory angle  $\theta_e = 45.62^\circ$  [see Eq. (18)].

#### D. Energy Resolution

Although the laboratory energies were measured to great precision,<sup>1</sup> there is a spread in center-of-mass energies, due to the zero-point vibrational motion of the hydrogen molecules,<sup>11</sup> which amounts to approximately 1 keV (full width). We have investigated the effect of smearing the theoretical cross section over this range and find that it is completely negligible, even though the minimum of the cross section is located to 0.1 keV (c.m.).

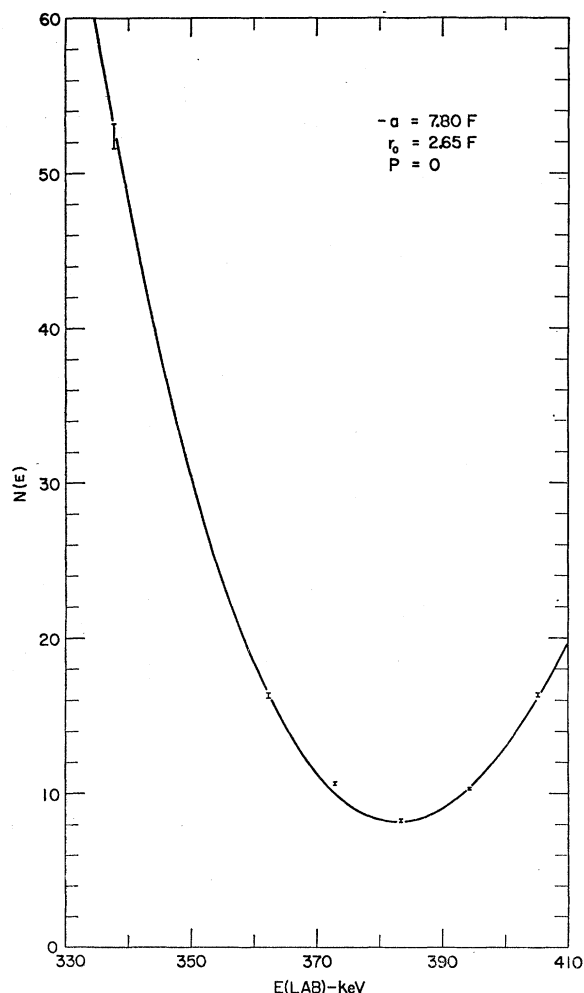


FIG. 5. The best fit to the data obtained by integrating the theoretical cross section, using the parameters shown on the figure, over the geometry of the experiment. Including or omitting the point at 373 keV results in best fits which are indistinguishable on the scale used here.

<sup>11</sup> We thank Dr. Critchfield for calling this point to our attention.

#### E. Results of Analysis of the Los Alamos Experiment

The parameters which enter the analysis fall into two categories: (i) the geometry factor  $I_2/I_0$ , and the shape parameter  $P$ , which are varied over specified ranges but are not searched upon; and (ii)  $\mathcal{E}$ ,  $\mathfrak{D}$ , and the normalization constant (which converts cross section to number of counts), which are searched upon for fixed values of the type (i) parameters.

A least-squares fit was performed, first omitting the data at 0.37283 MeV (see the discussion in Ref. 1 concerning this point). Choosing  $I_2/I_0$  equal to  $1.171 \times 10^{-4}$  (see Sec. C) and  $P=0$ , the optimum parameters are

$$\mathcal{E} = 0.38242 \quad \mathfrak{D} = 0.142$$

with  $\chi^2 = 3.48$  (two degrees of freedom). Inverting the

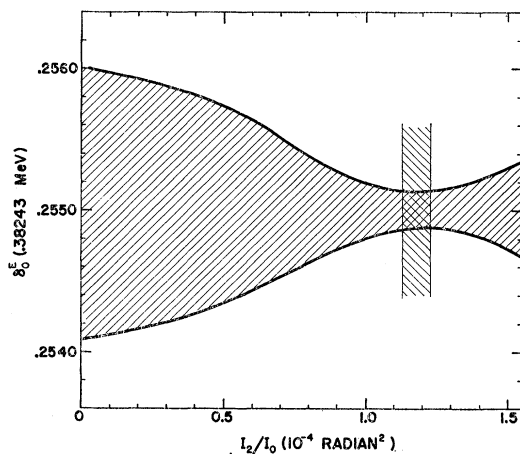


FIG. 6. For each assumed value of  $I_2/I_0$  (the normalized second moment of the angular weight function) the least-squares fit defines a range of acceptable values of the  $s$ -wave phase shift  $\delta_0^E$  at the energy 0.38243 MeV, shown with hachure. The vertical lines limit the permitted range of  $I_2/I_0$  and therefore the area of crossed hachure is the region of the plot which the geometry of the experiment (and multiple scattering) allows.

definitions (9) and (10) gives

$$a = -7.80 \text{ F}, \quad r_0 = 2.65 \text{ F}.$$

This fit to the data is shown on Fig. 5. Furthermore the energy at which  $\sigma(90^\circ)$  has its minimum is  $E_{\min} = 0.38243$  MeV, which is almost identical with  $\mathcal{E}$ , and the phase shift at 0.38243 MeV is  $\delta_0^E(0.38243) = 0.25501$ . Of course there is an error associated with each of these quantities, and this error will be enlarged by considering the whole range of acceptable values of  $I_2/I_0$  and  $P$ . We first vary  $I_2/I_0$  from  $1.13 \times 10^{-4}$  to  $1.22 \times 10^{-4}$  (see Sec. C), keeping  $P$  fixed at zero. This has an almost negligible effect upon all of the above parameters (and their errors) except  $\mathfrak{D}$  (which is poorly known). In Fig. 6 is plotted the variation of  $\delta_0^E(0.38243 \text{ MeV})$  with  $I_2/I_0$  over a much wider range, including  $(I_2/I_0) = 0$  which represents pure  $90^\circ$  scattering. The vertical lines limit

the acceptable range of  $I_2/I_0$ , and the two curves represent, for each value of  $I_2/I_0$ , the extreme values of  $\delta_0^E$  which the least-squares analysis defines. The area of crossed hachure is therefore the acceptable region of the plot, and it is seen that the uncertainty in the geometrical aspects of the calculation gives rise to an almost negligible additional uncertainty in the phase shift over what the statistics alone demand. It is also clear from Fig. 6 that including the finite geometry in the analysis makes a significant difference in the ability to pin down the phase shift.

A similar calculation is performed by varying  $P$  from  $-0.05$  to  $+0.10$  (see Sec. B) keeping  $I_2/I_0$  fixed at  $1.171 \times 10^{-4}$ . Again there is very little effect upon the best values of the parameters, but their uncertainties are increased. The effect upon  $\delta_0^E(0.38243 \text{ MeV})$  is shown on Fig. 7 where the two curves represent, for each value of  $P$ , the extreme values of  $\delta_0^E$  defined by the least-squares analysis.

The net effect of the variations in  $I_2/I_0$  and  $P$ , is the following set of parameters:

$$\begin{aligned} \mathcal{E} &= 0.38242 \pm 0.00026, \\ \mathfrak{D} &= 0.142 \pm 0.043, \\ E_{\min}(90^\circ) &= 0.38243 \pm 0.00020 \text{ MeV}, \\ \delta_0^E(0.38243 \text{ MeV}) &= 0.25501 \pm 0.00020 \end{aligned}$$

with 60% of the errors in  $E_{\min}$  and  $\delta_0^E$  coming from statistics, and almost all the remainder arising from the spread in  $P$ . If this data were analyzed simultaneously with data at slightly higher energies, then  $P$  could be searched upon as another parameter and this would very probably lower the errors given above. The result for  $E_{\min}$  agrees with the older experiment<sup>2</sup> but is much more accurate.

The scattering length and effective range are found to be

$$\begin{aligned} a &= -7.80 \pm 0.15 \text{ F} \\ r_0 &= 2.65 \pm 1.1 \text{ F}. \end{aligned}$$

As anticipated,  $a$  and  $r_0$  separately are determined very poorly from this experiment. Only the one linear combination  $\mathcal{E}$ , which is very accurately equal to the energy of the minimum of the  $90^\circ$  cross section, is determined well by the experiment. Indeed the entire uncertainty in  $a$  and  $r_0$  is due to the uncertainty in the orthogonal combination  $\mathfrak{D}$ .

If the less reliable<sup>1</sup> data at 0.37283 are included in the analysis, then (with  $I_2/I_0$  at its best value, and  $P=0$ )  $\delta_0^E(0.38243) = 0.25489$ , which is within the previously quoted error, but  $\chi^2 = 13.35$ . The one point in question contributes 7.40 to  $\chi^2$ . The statistical error alone on this phase shift is  $\pm 0.00018$ . This best fit is indistinguishable from the best fit which omits this point, on the scale used in Fig. 5. We choose as our final results those obtained without this point.

If the Coulomb parameter  $\eta$  is computed using a non-

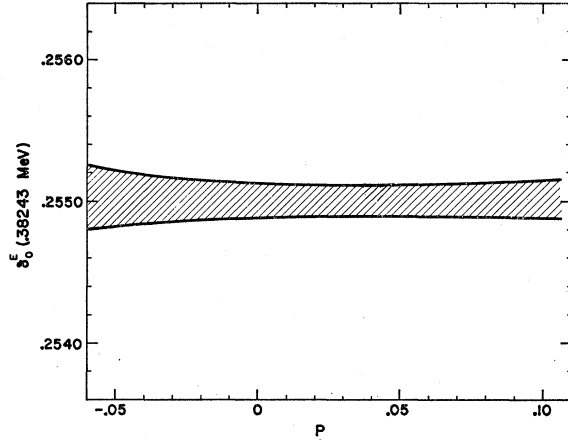


FIG. 7. For each assumed value of  $P$ , the least-squares fit defines a range of acceptable values of the  $s$ -wave phase shift  $\delta_0^E$  at the energy 0.38243 MeV, shown with hachure. The entire range of  $P$  shown was considered acceptable for the sake of evaluating the uncertainty in  $\delta_0^E$ .

relativistic calculation of the proton's laboratory velocity, then the phase shift is  $\delta_0^E(0.38243) = 0.25493$ , which is within the previously quoted error, and  $\chi^2$  is almost identical with the value obtained above. Since this value of  $\eta$  is even more removed from the value used above than what would have been obtained using twice the center-of-mass velocity of the incident proton (computed relativistically, see Ref. 7), it is clear that (as expected) this relativistic question is of practically no consequence at this energy, even for such an accurate experiment.

If the entire analysis is performed omitting vacuum polarization, then  $\delta_0(0.38243) = 0.25409$  and  $\chi^2$  is essentially unchanged from its value when vacuum polarization was included. This is as expected since, in general, it is not possible for cross sections over a very small energy and/or angular interval to distinguish whether or not vacuum polarization is present. Note, however, that the phase shift required to fit the data when vacuum polarization is omitted (written above with no superscript) is well outside the acceptable range for  $\delta_0^E$ .

From the method of admission of the hydrogen to the apparatus (see Fig. 4 of Ref. 1) the gas in the target area is expected to be below room temperature. A simple adiabatic expansion from 295°K and 3.65 Torr to 0.307 Torr would result in a temperature of 145°K. The actual temperature must be larger than this because the gas enters as a jet, and the directed velocity is rapidly randomized; in addition there is some conduction from the walls, and beam heating. Using the conversion factor, kindly supplied by Seagrave, that one unit of  $Q$  [see column ( $k$ ), Table I, Ref. 1] equals  $1.25 \times 10^{11}$  protons, and the fact that the normalization constant  $C'$  in Eq. (17) is  $37.8 \text{ F}^{-2}$  (as determined by the least-squares analysis), we find that the temperature

required for the target gas is 243°K, if the absolute value of the cross section is to be fit. In the sense that this temperature is between the crude limits stated above, there is no inconsistency.

### III. THE *s*-WAVE PHASE SHIFT UP TO 3 MeV

If the phase shift given above is combined with the four *s*-wave phase shifts obtained from the most recent very precise Wisconsin data<sup>3,4</sup> which extends from 1.4 to 3.0 MeV, then the discussion in Ref. 5 shows that one has enough information to expand the effective range function beyond the shape-independent approximation. The following caution must be exercised concerning the significance of the coefficients in this expansion.

The effective range function is an analytic function<sup>12</sup> of  $k^2$  in a region containing  $k^2=0$ , and therefore has a power series expansion, Eq. (6), convergent in some finite circle. If one fits some experimentally determined values of  $X$  using a second-order polynomial ( $k^4$  is the highest power), then are the coefficients so determined actually equal to the first three coefficients in the power series expansion? The answer is yes only if the higher terms in the power series are negligible at all of the experimental energies under consideration. One cannot decide this by just examining the experimentally determined phase shifts, which may have only enough information in them to enable three coefficients to be extracted. Rather, one must have some theoretical guidance as to whether or not the higher terms are negligible, e.g., by using a fairly realistic potential and seeing what it predicts for the higher terms.

Using some low-energy *s*-wave phase shifts computed by Signell,<sup>13</sup> which are the predictions of the Yale<sup>14</sup> and Hamada-Johnston<sup>15</sup> potentials, we find that the  $k^6$  term in the expansion is of comparable importance with the  $k^4$  term at 3 MeV. This means that a second-order polynomial fit to the experimental phase shifts will not yield the first three coefficients of the power series

TABLE II. Phase shifts used in effective range analysis.

$E_{\text{lab}}$ (MeV)	$\delta_0^E$ (deg)
0.38243	14.611±0.011
1.397	39.317±0.015
1.855	44.346±0.021
2.425	48.361±0.014
3.037	51.013±0.020

<sup>12</sup> See H. Cornille and A. Martin, *Nuovo Cimento* **26**, 298 (1962), and D. Y. Wong and H. P. Noyes, *Phys. Rev.* **126**, 1866 (1962) for the Coulomb-plus-nuclear case. We believe, but have not yet proven, that the effective range function employed in this paper which includes vacuum polarization is also analytic out to 10 MeV laboratory energy (corresponding to one pion exchange).

<sup>13</sup> We thank Dr. Signell for kindly supplying us with these phase shifts.

<sup>14</sup> K. E. Lassila, M. H. Hull, Jr., H. M. Ruppel, F. A. McDonald, and G. Breit, *Phys. Rev.* **126**, 881 (1962).

<sup>15</sup> T. Hamada and I. D. Johnston, *Nucl. Phys.* **34**, 382 (1962).

expansion. This must be kept in mind when efforts are made to compare the numbers obtained from a second-order polynomial fit to the predictions of some model. Rather than compare some intermediate quantities such as the effective range parameters, it would be better to compare the predicted phase shifts directly with the experimentally determined ones, or better still, the predicted cross sections with the experimental values.

Bearing in mind the restricted significance to be attached to the coefficients obtained from polynomial fits, we have made linear, quadratic, and cubic fits to the phase shifts. Table II shows the phase shifts which were used,<sup>16</sup> and Table III shows the results of the three fits along with their  $\chi^2$  values and probabilities.

It is seen that the data do not contain any information about  $Q$ , and also that the value of  $P$  obtained from the quadratic fit probably has very little to do with the actual coefficient of the  $k^4$  term in the power series expansion of the effective range function. To the extent that  $a$  and  $r_0$  are stable (against the effect of including higher powers of  $k^2$ ) one may assume that they correctly represent the coefficients of the constant and linear terms in the series expansion.

The linear and quadratic fits have been plotted on Fig. 8, along with the experimentally determined values of the effective range function using the phase shifts and uncertainties from Table II. To make the distinction between the linear and quadratic fits apparent, we subtracted at each energy the value of the linear fit from each quantity, and then plotted the results on a greatly expanded vertical scale. The linear fit itself therefore appears as a horizontal line through the value zero. It is plain from Fig. 8 that the experimentally determined values of the effective range function do exhibit curvature as a function of energy, of the type which goes with a positive value for the parameter  $P$ .

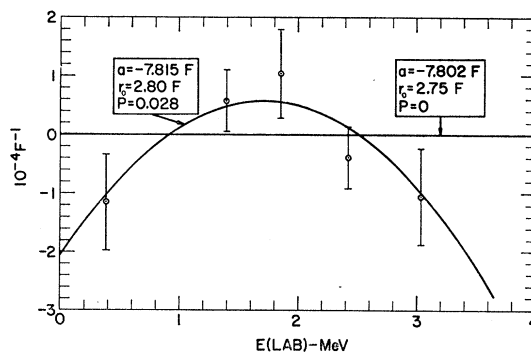


FIG. 8. Linear and quadratic fits to the five experimentally determined values of the effective range function. At each energy the value of the linear fit was subtracted from each quantity (linear fit, quadratic fit, and experimental value) and the results plotted on a greatly expanded vertical scale. The parameters associated with the two fits are shown.

<sup>16</sup> The four Wisconsin phases were taken from Ref. 4 using the relation  $K_0 = \delta_0^E + \tau_0$  and values of  $\tau_0$  from Ref. 5.



TABLE III. Effective range parameters obtained from three different polynomial fits to the five very accurate low-energy phase shifts.

Fit	$a(F)$	$r_0(F)$	$P$	$Q$	$\chi^2_{\text{fit}}$	$P(\chi^2 > \chi^2_{\text{fit}})$
Linear	$-7.802 \pm 0.005$	$2.745 \pm 0.006$	0	0	5.9	0.12
Quadratic	$-7.815 \pm 0.008$	$2.795 \pm 0.025$	$0.028 \pm 0.014$	0	1.74	0.42
Cubic	$-7.823 \pm 0.012$	$2.866 \pm 0.078$	$0.114 \pm 0.093$	$0.17 \pm 0.18$	0.81	0.37

Although  $P$  is now delimited considerably better than the range which was permitted in Part II of the paper we have not gone back to reduce the errors quoted there, partly to keep the results of that analysis independent of the higher energy experiments, and also in an attempt to take some cognizance of the 'bad' point at 0.37283 MeV. We do not know the proper way to do this, but think that the enlarged errors used in Part II should be kept partly for this reason.

If the quadratic-fit parameters obtained above are used at 9.69 MeV, 90°c.m., with the same  $p$ -wave assumptions as before, namely, one pion exchange tensor force and no spin-orbit force, the result is  $\sigma_{\text{e.m.}} = 55.0$  mb/ster, compared with the experimental value<sup>17</sup> of  $54.6 \pm 0.4$  mb/ster. This good agreement further demonstrates the distinction between a polynomial fit with a few terms and a power series, because the power series expansion of the effective range function is known to diverge<sup>12</sup> beyond 10 MeV, and therefore the first three terms of the series are not likely to be a good approximation to the entire series at 9.69 MeV.

#### IV. CONCLUSIONS

An analysis of cross-section data<sup>1</sup> near 90°c.m. (omitting the point at 0.37283 MeV) located the minimum of the 90° cross section at  $E_{\text{min}} = 0.38243 \pm 0.00020$  MeV, and the nuclear  $s$ -wave phase shift was evaluated:  $\delta_0^E = 0.25501 \pm 0.00020$  at the precise energy 0.38243 MeV. Sixty percent of these uncertainties come from the statistics and most of the remainder from a permitted spread in the parameter  $P$  which was not searched upon. If the point at 0.37283 MeV (see discussion in Ref. 1 about this point) is included in the analysis a poor statistical fit is obtained, but the phase shift is within the error quoted above. In the course of studying the effect of the geometry of the experiment<sup>1</sup> and multiple scattering upon the results it was found that the effective angle is  $\theta_{\text{e.m.}} = 91.24^\circ$ , i.e.,  $N(E)$  in Table I is proportional to the cross section at this angle.

When the phase shift given above is combined with the four recent phase shifts obtained from Wisconsin data<sup>3,4</sup> which extend from 1.4 to 3.0 MeV, it is found that a quadratic fit to the effective range function is definitely superior to a linear fit, and the parameters of the former fit are:  $a = -7.815 \pm 0.008$  F;  $r_0 = 2.795 \pm 0.025$  F; and  $P = 0.028 \pm 0.014$ . Consideration of some realistic potentials shows that the next term ( $k^6$ )

in the expansion of the effective range function is of comparable importance with the  $k^4$  term at 3 MeV, and therefore the parameters of the quadratic fit are not necessarily the ones associated with the power series expansion of the effective range function. The comparative stability of  $a$  and  $r_0$  as higher powers of  $k^2$  are introduced indicate that their values are quite close to the corresponding coefficients in the first two terms of the power series, but  $P$  may be quite different from the actual coefficient occurring in the  $k^4$  term.

Nevertheless one can use the quadratic fit as an accurate method for predicting the  $s$ -wave phase shift at low energies, and even at 9.69 MeV good agreement with the experimental<sup>17</sup> 90° cross section is obtained.

#### ACKNOWLEDGMENTS

We thank Dr. Brolley and Dr. Seagrave for several detailed discussions about their experiment, and for providing us with the information needed in this analysis. Dr. Dahl and Dr. Knecht kindly supplied us with the most recent information about the Wisconsin data. Discussions and correspondence with Dr. Noyes have been very helpful and stimulating.

#### APPENDIX A: EMPIRICAL FORMULAS FOR VACUUM POLARIZATION QUANTITIES

The first set of three formulas refer to the quantities which enter the  $s$ -wave effective range expansion. They are accurate to better than 1% in the energy range  $0.1 < E < 4.2$ , where  $E$  is the laboratory energy in MeV, and  $\ln$  is the natural logarithm.

$$\begin{aligned} \tau_0 = & -1.59167 \times 10^{-3} + 3.00470 \times 10^{-4} \ln E \\ & + 3.02177 \times 10^{-5} \ln^2 E - 2.16455 \times 10^{-5} \ln^3 E \\ & + 3.73036 \times 10^{-6} \ln^4 E, \end{aligned}$$

$$\begin{aligned} \chi_0 = & -1.51975 \times 10^{-3} + 5.97111 \times 10^{-4} \ln E \\ & - 1.12282 \times 10^{-4} \ln^2 E + 5.49672 \times 10^{-6} \ln^3 E \\ & + 5.05571 \times 10^{-6} \ln^4 E, \end{aligned}$$

$$\begin{aligned} I_0 = & -2.66203 \times 10^{-3} + 5.48719 \times 10^{-5} \ln E \\ & + 2.95002 \times 10^{-4} \ln^2 E - 4.52868 \times 10^{-6} \ln^3 E \\ & - 8.35377 \times 10^{-6} \ln^4 E. \end{aligned}$$

The next set of formulas calculate the real and imaginary parts of the (unsymmetrized) vacuum polarization scattering amplitude. The formulas are presented in the form of corrections to the amplitude calculated by Durand.<sup>18</sup> These corrections vanish as the

<sup>17</sup> L. H. Johnston and D. E. Young, Phys. Rev. **116**, 989 (1959).

<sup>18</sup> L. Durand, III, Phys. Rev. **108**, 1597 (1957).

energy increases. The numbers within the quotation marks are equation numbers in Durand's paper.<sup>18</sup>

$$\nu \equiv 2\kappa^2/k^2; (2\kappa)^{-1} = \hbar/2mc = 193.1 \times 10^{-13} \text{ cm},$$

$\theta$  is center-of-mass scattering angle,

$$x \equiv \cos\theta,$$

$$\text{Re}[kf_{v.p.}(\theta)] = [{}^{12.2} + {}^{19.2} + {}^{20}]$$

$$\times \left[ 1 + (2.6843 - 2.3237x - 0.912x^2) \right. \\ \left. \times 10^{-2} \left( \frac{\eta}{0.255161} \right)^{2.4} \right],$$

$$\text{Im}[kf_{v.p.}(\theta)]$$

$$= {}^{19.1} + [-6.9231 - 3.6319x - 8.3669x^2 - 7.2723x^3] \\ \times 10^{-5} \left( \frac{\eta}{0.255161} \right)^{2.9}.$$

$F(x)$  in "12.2" is obtained from "12.3" and "12.4".

These amplitude formulas are valid above 200 keV with the following restrictions on angle:

At  $E \geq 1.4$  MeV, the corrections are all small and should be set equal to zero forward of  $20^\circ$ .m. The uncorrected formulas are good between  $10^\circ$  and  $20^\circ$ .

At  $E = 0.4$  MeV, the corrections are no good forward of  $30^\circ$ .

#### APPENDIX B: THE $90^\circ$ COULOMB AND NUCLEAR $s$ -WAVE AMPLITUDES

A simple physical picture of the main features of the low-energy scattering amplitude at  $90^\circ$ .c.m. can be gotten if vacuum polarization is omitted from consideration. For then the symmetrized (singlet) nuclear amplitude (assumed to be pure  $s$ -wave) can be written as

$$\frac{1}{2}kf_N = \sin\delta e^{i\delta}, \quad (\text{B1})$$

where  $\delta$  is the  $s$ -wave phase shift. The symmetrized (singlet) Coulomb amplitude at  $90^\circ$ .c.m. is

$$\frac{1}{2}kf_c(90^\circ) = -\eta e^{i\eta \ln 2}. \quad (\text{B2})$$

As the real number  $\delta$  increases from zero (with increasing energy)  $\sin\delta e^{i\delta}$  moves in the complex plane, along the arc of a circle whose center is at  $0.5i$  and whose radius is 0.5. This is shown on Fig. 9. As the real number  $\eta$  decreases (with increasing energy),  $\eta e^{i\eta \ln 2}$ , which from Eq. (B2) is proportional to the negative of the  $90^\circ$  Coulomb amplitude, moves inward along an Archimedes spiral in the complex plane. This is also shown on

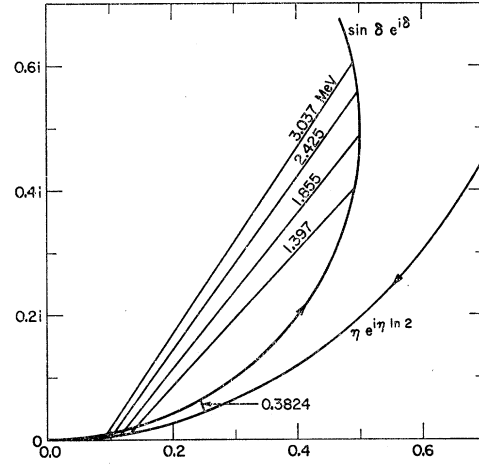


Fig. 9. The complex plane showing  $\frac{1}{2}k$  multiplied by the symmetrized singlet nuclear  $s$ -wave amplitude and the same thing for the negative of the  $90^\circ$  Coulomb amplitude. The straight line segments, labeled with the laboratory energy of the incident proton, connect corresponding points on the two curves and represent  $\frac{1}{2}k$  multiplied by the sum of the Coulomb and nuclear amplitudes. The arrows show how the points move with increasing energy.

Fig. 9. For a given value of the energy,  $\eta$  has a definite value corresponding to a fixed point on the spiral. The nuclear-physics problem is to determine where one is on the circle for that same value of the energy, i.e., what  $\delta(E)$  is. A straight line connecting the two points in question would be proportional to the sum of the nuclear and Coulomb amplitudes, since  $\eta e^{i\eta \ln 2}$  is proportional to the negative of the Coulomb amplitude. Even without knowing the exact variation of  $\delta$  with  $E$ , just from the knowledge that the nuclear and Coulomb points are moving in opposite directions it is clear that there will be an energy at which the two points will 'pass by' each other, giving a minimum in the total amplitude. If this occurs at a small value of  $\eta$  then  $\delta \approx \eta$  at the minimum. This result has been known for a long time.<sup>2,19</sup>

One can refine this estimate by examining the geometry of Fig. 9 more closely, but the result will be altered when vacuum polarization is included. The analysis given in the body of the paper shows that at the minimum of the  $90^\circ$  cross section (0.3824 MeV),  $\eta = 0.2557$  and  $\delta_0/E = 0.2550$ . These two points have been connected on Fig. 9 with a straight line segment which is labeled with the energy. The same thing has been done for the four Wisconsin energies, and the resulting picture of how the total  $90^\circ$  amplitude varies with energy, provides a somewhat deeper understanding of the variation of the  $90^\circ$  cross section shown on Fig. 1.

<sup>19</sup> H. A. Bethe and P. Morrison, *Elementary Nuclear Theory* (John Wiley & Sons, Inc., New York, 1956), 2nd ed., pp. 95-96.